# Oscillating behavior of a compartmental model with retarded noisy dynamic infection rate

Michael Bestehorn, Thomas M. Michelitsch

# Oscillating behavior of a compartmental model with retarded noisy dynamic infection rate

Michael Bestehorn

*Brandenburgische Technische Universität Cottbus-Senftenberg,*

*Institut für Physik,*

*Erich-Weinert-Straße 1,*

*03046 Cottbus, Germany*

*bestehorn@b-tu.de*

Thomas M. Michelitsch

*Sorbonne Université, Institut Jean le Rond d'Alembert,*

*CNRS UMR 7190, 4 place Jussieu, 75252 Paris cedex 05, France*

*thomas.michelitsch@sorbonne-universite.fr*

# Abstract

Our study is based on an epidemiological compartmental model, the SIRS model. In the SIRS model, each individual is in one of the states susceptible (S), infected(I) or recovered (R), depending on its state of health. In compartment R, an individual is assumed to stay immune within a finite time interval only and then transfers back to the S compartment. We extend the model and allow for a feedback control of the infection rate by mitigation measures which are related to the number of infections. A finite response time of the feedback mechanism is supposed that changes the low-dimensional SIRS model into an infinite-dimensional set of integro-differential (delay-differential) equations. It turns out that the retarded feedback renders the originally stable endemic equilibrium of SIRS (stable focus) into an unstable focus if the delay exceeds a certain critical value. Nonlinear solutions show persistent regular oscillations of the number of infected and susceptible individuals. In the last part we include noise effects from the environment and allow for a fluctuating infection rate. This results in multiplicative noise terms and our model turns into a set of stochastic nonlinear integro-differential equations. Numerical solutions reveal an irregular behavior of repeated disease outbreaks in the form of infection waves with a variety of frequencies and amplitudes.



Keywords: Epidemic models, delay-differential equations, stochastic differential equations, bifurcation theory, numerical simulations, stability analysis

## I. INTRODUCTION

Mathematical modeling of epidemic dynamics goes back to the seminal work of Kermack and McKendrick [1927] where the nowadays called 'SIR model' was introduced, an acronym from (**S** = susceptible, **I** = infected, **R** = recovered). The basic SIR model and its various extensions (for a review see [1, 16]) are also called 'compartmental models' since they divide the individuals into several compartments depending on their state of health. It turned out that the features of infectious diseases such as measles, mumps, and rubella could to a certain extend be captured by such simple models. A huge field has emerged to describe epidemic spreading in the framework of random walks in complex networks [5, 6, 19, 20] and (generalized) fractional dynamics [17, 18, 22], just to name but a few. A model based on a small world network is discussed in [23, 24] and proved to be superiour to SIR (or SEIR) models comparing its results with data provided by the SARS outbreak in mthe year 2003.

Time periodic outbreaks have been noticed for a long time in the dynamics of several diseases and were already stated in 1929 by Soper in a model for the time evolution of measles cases [25].

The SIR model and most of its extensions are not able to describe sustained oscillations but rather account for a single outbreak caused by the instability of the disease free state. In the long time limit, the endemic equilibrium is reached where the fractions of the population in the different compartments attain constant values. In the language of dynamical systems this behavior is known as a heteroclinic orbit, connecting in phase space an unstable fixed point (healthy state) with a stable one (endemic state). In the following we shall consider an extended SIRS model where the time of immunity is finite and in the endemic equilibrium a nonzero number of infected individuals remains present so that the disease never become extinct completely. In the original SIR or SIRS models, the interplay between infected and susceptible individuals is inspired by the dynamics of the even older predator-prey systems [14] and is expressed in the form of a simple bilinear term $\beta_0\, I(t)\, S(t)$, where $I(t)$ and $S(t)$ are the number of infected and susceptible individuals and $\beta_0$ is the constant probability of infection at each contact (infection rate). The predator (infected) 'catches' the prey (susceptible) by infection.

Other work [13] considered a nonlinear infection rate according to

$$W = \beta(j)\, I(t)\, S(t) = \frac{\beta_0\, I^m(t)\, S(t)}{1 + \alpha I^n(t)} \ , \tag{1}$$

and obtain limit cycle solutions for certain parameters $m = n \geq 2,\ \alpha > 0$. Tang et al. [2008] studied the case $m = n = 2$ and found a weak focus and the existence of two limit cycles. For $m \geq n$, $W$ is a monotonically increasing function of $I$ that saturates for $m = n$. For $m = n = 1$ the dynamics is qualitatively the same than for the standard SIR model and sustained oscillations cannot be observed. The denominator $1 + \alpha I^n$ accounts for mitigation measures against the epidemics that naturally increase with increasing $I$. We only note that for the case $n > m$ the interaction $W$ has a maximum at a certain infection number. For such nonmonotonic behavior it was shown in [28] that the dynamics in the long time limit approaches a stable fixed point as for the original SIR or SIRS models.

In the present paper we want to stay as close as possible at the standard SIRS model and will not consider additional limit cycle solutions obtained for $m = n \geq 2$ or non-monotonic functions $W$ of $I$. We therefore study a SIRS model with the most simple nonlinear interaction of the form (1) with $m = n = 1$. Taking the recent Covid epidemic as an example, such a feedback control is realized by certain containment measures like social distancing, hygiene rules, or wearing masks. Normally these measures take effect after a certain retardation that can be on the same time scale or even much longer than the time of recovery. The time delay can be either distributed or singular. In our model we generalize (1) by replacing $I(t)$ in the feedback by a memory integral as follows

$$W = \frac{\beta_0\, I(t)\, S(t)}{1 + \alpha I_d(t)} \quad \text{with} \quad I_d(t) = \int_{-\infty}^{t} K(t-\tau) I(\tau) \mathrm{d}\tau \ . \tag{2}$$

For the distributed case, $K(t)$ is a given causal normalized probability density function (PDF) introducing memory into the model. The singular time delay is a special case with $K(t-\tau) = \delta(t - \tau - \tau_0)$ with Dirac's $\delta$-function.

Delay or memory terms were introduced in epidemiological models by many other researchers, for an overview see [21]. In a previous work we considered a SIRS model with a retarded transition from the R to the S compartment, reflecting the rather long time of decay of immunity [6]. From the mathematical point of view, the presence of a delay term in an ordinary differential equation makes a low-dimensional system infinitely dimensional and may allow for the occurrence of periodic, quasi-periodic or even chaotic behavior, rendering

the dynamics much more complex [3, 10, 15]. Memory effects introduced by finite incubation periods, delayed infectiousness and the distribution of the recovery period are considered in an upcoming paper [2].

The main focus of the present paper is to analyze an epidemiological model that allows for persistent periodic outbreaks of the disease, in contrast to the standard SIR or SIRS models that show an asymptotically constant endemic equilibrium. To simulate environment fluctuations, noise terms are added that may have a significant influence of the amplitude and period of the oscillations.

The paper is organized as follows: After introducing the modified SIRS model with retarded feedback control in part II, we perform in part III a local linear stability analysis close to endemic equilibrium. Threshold parameters are determined for which the endemic equilibrium becomes oscillatory (Hopf) unstable. The existence of a Hopf unstable endemic equilibrium is crucial for the occurrence of sustainable periodic outbreaks. For the kernel in (2) we consider a $\delta$-function and especially an Erlang PDF which contains two free parameters and turned out to be flexible enough to capture real-life situations [6]. In Part IV, fully nonlinear solutions for these cases are given above threshold and the occurrence of persistent oscillations around the endemic equilibrium is observed. Finally, noise terms are introduced into the infection rate, accounting for a fluctuating environment [7]. It is demonstrated that these terms are responsible for much more irregular oscillations, showing the typical behavior known from real-life data.

## II. MODEL

### A. SIRS model with feedback control

Let $S$, $I$, $R$ be the number of susceptible, infected, and recovered individuals, respectively and $N = S + I + R$ their total number. Assuming a bilinear interaction between susceptible and infected individuals, the SIRS model has the form

$$\frac{dS}{dt} = -\frac{\beta_0}{N} I\, S + \nu\, R \tag{3a}$$

$$\frac{dI}{dt} = \frac{\beta_0}{N} I\, S - \gamma\, I \tag{3b}$$

$$\frac{dR}{dt} = \gamma\, I - \nu\, R\ , \tag{3c}$$

where $\beta_0$ is the average number of contacts per individual per time, multiplied by the probability of disease infection between a susceptible and an infectious individual, and $1/\gamma$ is the average time of being infectious or the time of recovery. The parameter $\nu$ is the immunity loss rate and accounts for a finite life time of immunity $1/\nu$. For $\nu = 0$ the standard SIR model [11] is recovered.

Since no birth or death processes are considered in (3), the total number of individuals $N$ is constant in time. Instead of the numbers $S, I, R$ we introduce the fractions $s(t), j(t), r(t) \in [0, 1]$

$$s(t) = \frac{S(t)}{N}, \quad j(t) = \frac{I(t)}{N}, \quad r(t) = \frac{R(t)}{N} \tag{4}$$

and obtain from (3)

$$\frac{ds}{dt} = -\beta_0\, j\, s + \nu\, r \tag{5a}$$

$$\frac{dj}{dt} = \beta_0\, j\, s - \gamma\, j \tag{5b}$$

$$\frac{dr}{dt} = \gamma\, j - \nu\, r\ , \tag{5c}$$

Scaling the time with $\gamma$ and considering $r + j + s = 1$, the system (5) is reduced to the nondimensional form

$$\frac{ds}{dt} = -R_0(j)\, j\, s + \mu\,(1 - j - s) \tag{6a}$$

$$\frac{dj}{dt} = R_0(j)\, j\, s - j\ , \tag{6b}$$

with $\mu = \nu/\gamma$ and

$$R_0(j) = \frac{\beta(j)}{\gamma}$$

as the basic reproduction number. From here we allow for an infection number dependent infection rate $\beta(j)$ to model feedback control by mitigation measures, see eq. (1). For arbitrary $R_0(j)$, the system (6) has a fixed point

$$j_h = 0, \quad s_h = 1\ , \tag{7}$$

corresponding to the disease free state and becoming unstable for $R_0(0) > 1$. For constant $R_0 > 1$, the other fixed point

$$j_e = \frac{\mu(R_0 - 1)}{R_0(\mu + 1)}, \quad s_e = \frac{1}{R_0} \tag{8}$$

denotes the endemic equilibrium and is unconditionally stable. Note that for $\mu = 0$, (8) turns into $j_e = 0,\ s_e = 1 - r_e$, where $r_e$ depends on the initial conditions and on the dynamics.

If containment measures take effect the infection rate $\beta$ will decrease. Since the strength of the measures normally increases with the number of infected individuals, it is nearby to assume a certain dependence $\beta = \beta_0/f(j)$ or

$$R_0(j) = \frac{r_0}{f(j)}, \qquad r_0 = \beta_0/\gamma \tag{9}$$

and $f(j) \geq 1$ as a monotonically increasing function of $j$ with $f(0) = 1$. The endemic equilibrium is now found from the solution of

$$j_e\,(1+\mu) + \frac{\mu f(j_e)}{r_0} - \mu = 0 \tag{10}$$

and depends on $f$. Taking the most simple form (2)

$$f(j) = 1 + \alpha j, \qquad \alpha \geq 0\ , \tag{11}$$

eq. (10) is linear in $j_e$ and

$$j_e = \frac{\mu(r_0 - 1)}{r_0(\mu+1) + \alpha\mu}, \quad s_e = \frac{1}{r_0}\ (1 + \alpha j_e)\ . \tag{12}$$

The infection number of the endemic equilibrium is monotonically decreasing with increasing $\alpha$ due to the containment measures. It exists again only for $r_0 > 1$ where it is proved to be always stable. for $r_0 > 1 + \mu/4 + O(\mu^2)$ the endemic equilibrium is a stable focus. For $r_0 \gg 1$, $j_e$ reaches the saturation value $\mu/(1+\mu)$ independent on $f$.

### B. Retarded infection rate control

The containment measures are not instantaneously coupled to the number of infected but follow them rather with a certain time delay. To include this issue, we introduce the causal probability density function (PDF) $K(\tau)$ from which the finite time of delay between cause and effect is drawn. Instead of (9) we may formulate

$$R_0(j) = \frac{r_0}{f(j_d(t))} \tag{13}$$

with the retarded infection

$$j_d(t) = \int_{-\infty}^{t} K(t-\tau) j(\tau) \mathrm{d}\tau\ . \tag{14}$$

The delay-time PDF is normalized,

$$\int_0^\infty K(t)\mathrm{d}t = 1.$$

The complete model reads

$$\frac{ds}{dt} = -\frac{r_0\, j\, s}{f(j_d)} + \mu\,(1-j-s) \tag{15a}$$

$$\frac{dj}{dt} = \frac{r_0\, j\, s}{f(j_d)} - j\ . \tag{15b}$$

Its solutions are defined by the control parameters $r_0,\ \mu$ and depend also on the form of $f(j)$ and $K(t)$. Due to the memory term, the initial conditions have to be extended to

$$s(0), \quad j(t),\ -\infty < t \leq 0$$

if the memory is infinite. In practice however, the memory has a finite length $t_0$ where $K(t > t_0) \to 0$. Then it is sufficient to integrate in (14) from $t - t_0$ to $t$ and fix the initial conditions for $j(t)$ on the stripe $-t_0 < t \leq 0$.

## III. STABILITY OF THE ENDEMIC EQUILIBRIUM

### A. Characteristic equation

For the rest of the paper we assume $f$ given as (11). To investigate the stability of the endemic equilibrium, we insert

$$s = s_e + u\,\mathrm{e}^{\lambda t}, \quad j = j_e + v\,\mathrm{e}^{\lambda t}$$

into (15) and linearize with respect to $(u, v)$. The solvability condition reads

$$P(\lambda) = a\lambda^2 + \lambda\,\left(r_0 + \alpha\tilde{K}(\lambda) + a\mu\right) + r_0\,(1+\mu) + \mu\alpha\,\tilde{K}(\lambda) = 0\ , \tag{16}$$

where $\tilde{K}(\lambda) = \int_0^\infty \exp(-\lambda t)K(t)dt$ stands for the Laplace transform of $K(t)$ and $a = 1+1/j_e$ with $j_e$ from (12). Since $\alpha, a, \mu, r_0 > 0$ and $\tilde{K}(0) = 1$, there exists no real valued $\lambda = 0$ as solution of (16). As a consequence, the endemic equilibrium (12) can only become unstable due to an oscillatory (Hopf) instability.

### B. $\delta$-kernel

Now we need to define the memory kernel. The most simple form is

$$K(t) = \delta(t - \tau_0)$$

where $\tau_0$ is the singular delay time between cause (high incidence) and effect (measures become active) and $\tilde{K}(\lambda) = \exp(-\lambda\tau_0)$. Inserting $\lambda = i\omega$, (16) is separated into real and imaginary parts and a quadratic equation for the Hopf frequency $\omega^2$ can be derived:

$$a^2\omega^4 + \omega^2\left(r_0^2 + a^2\mu^2 - \alpha^2 - 2r_0a\right) + r_0^2(1+\mu)^2 - \alpha^2\mu^2 = 0 \tag{17}$$

from where $\omega$ is determined from the larger root. Finally, $\tau_0$ follows from

$$\tau_0 = \frac{1}{\omega}\arccos\left(\frac{-r_0(\mu(1+\mu)+\omega^2)}{\alpha(\mu^2+\omega^2)}\right) . \tag{18}$$

Fig.1 shows $\tau_0$ and the time period $2\pi/\omega$ for which the fixed point $j_e, s_e$ becomes oscillatory unstable as a function of $r_0$ for fixed $\alpha = 50$ and $\mu = 0.1$.

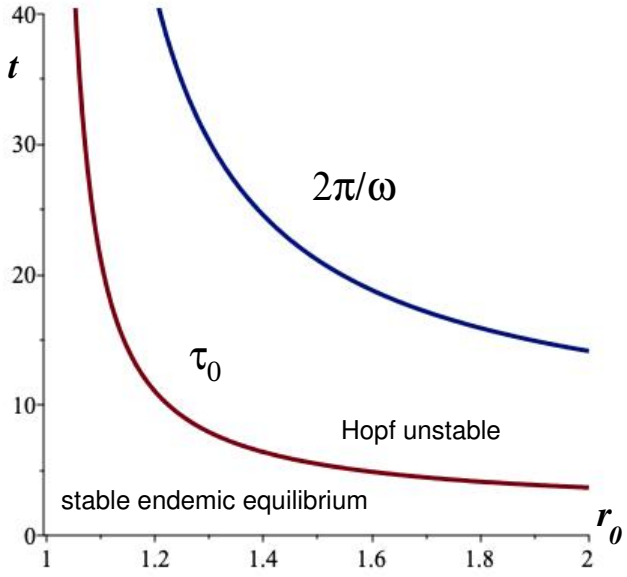


FIG. 1: $\tau_0$ and $2\pi/\omega$ according to (17,18) as a function of $r_0$ for $\alpha = 50$ and $\mu = 0.1$. Time in units of the recovery time $1/\gamma$. Above the red line the endemic equilibrium is oscillatory unstable.

### C. Erlang kernel

Another candidate for the kernel which is able to capture a variety of behaviors is the so called Erlang distribution (also called gamma-distribution) which has the form

$$K_{\eta,\xi}(t) = \frac{\xi^\eta t^{\eta-1}}{\Gamma(\eta)} e^{-\xi t}, \quad \eta > 0, \quad \xi > 0, \quad t \geq 0 \ , \tag{19}$$

where the index $\eta$ may take any positive (including non-integer) values and $\Gamma(\eta)$ denotes the Euler Gamma-function which recovers the standard factorial $\Gamma(\eta+1) = \eta!$ when $\eta \in \mathbb{N}_0$.

The Erlang distribution (19) contains two parameters $\eta,\ \xi > 0$ which may take any positive values. The Erlang PDF has the Laplace transform

$$\hat{K}_{\eta,\xi}(\lambda) = \int_{-\infty}^{\infty} e^{-\lambda t} \Theta(t) K_\eta(t) \mathrm{d}t = \frac{\xi^\eta}{(\xi+\lambda)^\eta} \ , \tag{20}$$

where $\Theta(t)$ indicates the Heaviside unit step function which comes into play by causality. The Erlang distribution is able to capture a variety of pertinent situations. For $\eta = 1$ the exponential PDF is recovered. Further the two extreme cases of a globally sharp time of immunity $\tau_0 = \eta/\xi$ as well as a broadly scattered distribution can be described. A sharp expected immunity life time $\tau_0$ is obtained by the limit

$$\lim_{\xi\to\infty} K_{\xi\tau_0,\xi}(t) = \delta(t-\tau_0). \tag{21}$$

where $\tau_0$ is constant. This feature can easily be seen by performing this limit in Fourier space, replacing in (20) the Laplace variable with $\lambda = i\omega$, thus

$$\lim_{\xi\to\infty} (1+i\omega/\xi)^{-\xi\tau_0} = e^{-i\omega\tau_0} = \int_{-\infty}^{\infty} e^{-i\omega t} \delta(t-\tau_0) \mathrm{d}t$$

which is the Fourier transform of Dirac's $\delta$-distribution $\delta(t-\tau_0)$. A broadly scattered distribution is obtained for $\hat{K}_{\eta,\xi}(\lambda) \to 0+$ for $\lambda > 0$ whereas $\hat{K}_{\infty,\xi}(0) = 1$ (normalization) is maintained. In this situation the parameters are chosen such that the Erlang variance is diverging

$$\langle (\Delta t)^2 \rangle = \frac{\eta}{\xi^2} \to \infty \ .$$

For $0 < \eta \leq 1$ the Erlang distribution is completely monotonic, for $\eta > 1$ it possesses a maximum at $t_m = (\eta-1)/\xi$. The Erlang PDF has a finite mean (expected response time of measures) $\langle t \rangle = \int_0^\infty t K_{\eta,\xi}(t) = \eta/\xi$, i.e. large $\eta$ and small $\xi$ increase the response time.

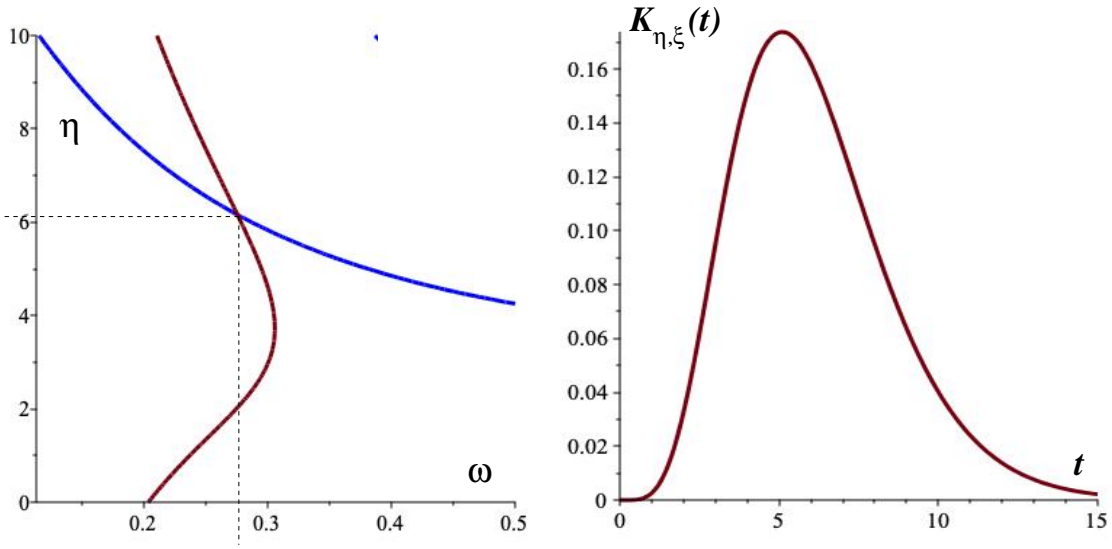


FIG. 2: Left: the zeros of imaginary part (blue) and real part of $P(i\omega)$ intersect at $\omega \approx 0.28$ and $\eta \approx 6.1$ for $\xi = 1,\ r_0 = 1.6$ and other parameters as in fig.1. Right: Erlang distribution for $\eta = 6.1,\ \xi = 1$.

Inserting (20) into (16), an analytic solution for $\omega$ is no longer accessible. Instead we propose a graphical solution by plotting the zero contours of real and imaginary parts of $P(i\omega)$ in the $(\omega, \eta)$ plane and looking for their intersections (fig.2). Thus, for fixed $r_0$ and $\xi$ a minimal value of $\eta$ for the instability of the endemic state as well as the Hopf frequency can be determined.

At $r_0 = 1.6$ and $\xi = 1$ we see from fig.2 a minimal value of $\eta \approx 6.1$. In this case the Erlang distribution has its maximum at $t_m \approx 5.1$.

## IV. NUMERICAL SOLUTIONS

### A. Deterministic model

#### *1. δ-kernel*

The system (15) is solved numerically by a 4th order Runge-Kutta method with fixed time step $\delta t = 0.001$ [4]. For the $\delta$-kernel, the last $n = \tau_0/\delta t$ values of $j$ are stored to compute the delay term. Fig.3 shows the number of infectious and the actual effective reproduction

number

$$R^{\rm eff}(t) = \frac{r_0\, s(t)}{1 + \alpha j_d(t)} \tag{22}$$

over time $t$. For $r_0 = 1.6$ the endemic equilibrium becomes unstable for $\tau_0 > 4.9$ with the Hopf frequency $\omega = 0.33$. If $\tau_0$ is increased, the oscillations become more and more anharmonic, their frequency decreases and their amplitude increases significantly, together with the mean values of $j$. We find

$$< j >= j_e = 0.009 \ (\tau_0 < 4.9), \quad < j >= 0.01 \ (\tau_0 = 5.2), \quad < j >= 0.012 \ (\tau_0 = 6.2) \ .$$

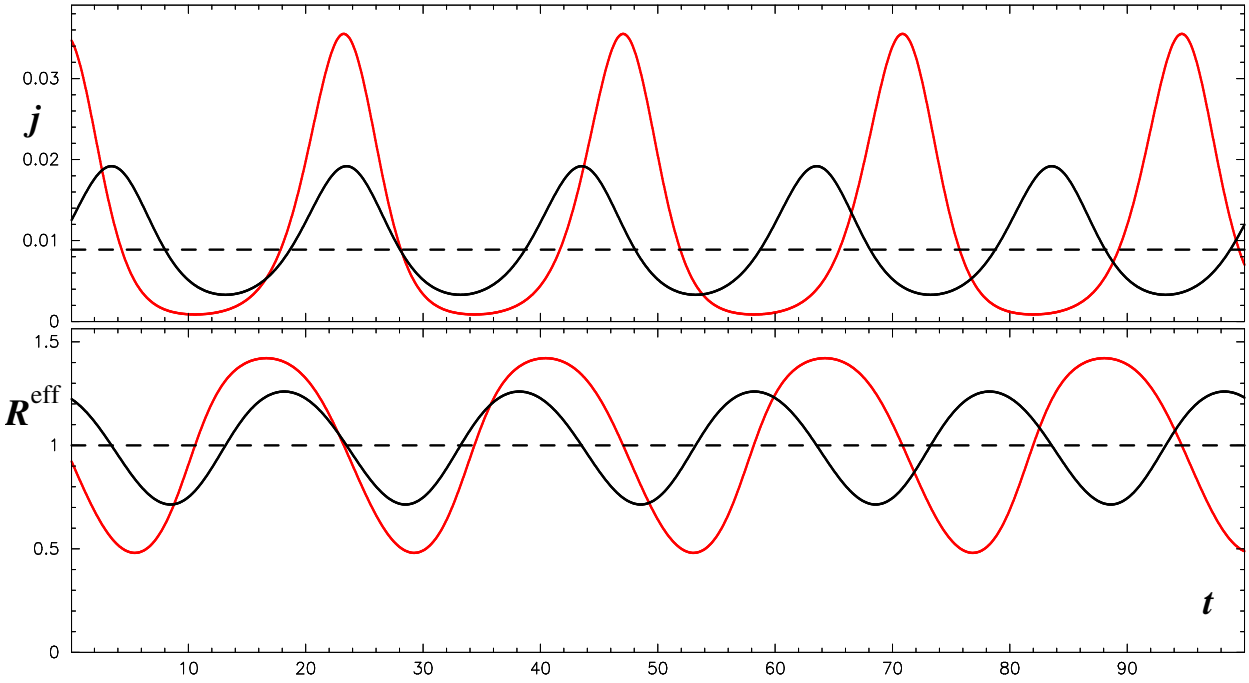


FIG. 3: Top: $j(t)$ over time for (15) with delta-kernel $K(t) = \delta(t - \tau_0)$, dashed line is the endemic equilibrium $j_e$. Bottom: effective reproduction number. Parameters as in fig.1, $r_0 = 1.6$, $\tau_0 = 5.2$ (black) and $\tau_0 = 6.2$ (red). Time in units of the recovery time $1/\gamma$.

*2. Erlang kernel*

Taking the Erlang distribution, the memory integral (14) must be approximated with a finite lower limit

$$j_d(t) = \int_{t-t_0}^{t} K(t-\tau) j(\tau) \mathrm{d}\tau \ . \tag{23}$$

and numerically evaluated by a sum over the last $n = t_0/\delta t$ time steps. We chose $t_0 = 5\,t_m$ where $t_m$ denotes the maximum of $K(t)$, resulting in an error in the order of $K(t_0)/K(t_m) \approx 2 \cdot 10^{-6}$. For the largest $\eta = 7$ we have $n = 30\,000$. Fig.4 shows the number of infectious and the actual effective reproduction number for this case, again for the parameters of (3) for $\eta = 6.5$ and $\eta = 7.0$. From the linear theory onset of oscillations is expected at $\eta \approx 6.2$, compare fig.2. The results are at least qualitatively similar to those of the $\delta$-kernel. This is due to the fact that the Erlang distribution for $\eta \approx 6$ has a pronounced and rather sharp maximum, cmp. fig.2, left frame. On the other hand, a monotonically decreasing kernel would not lead to an oscillatory instability.

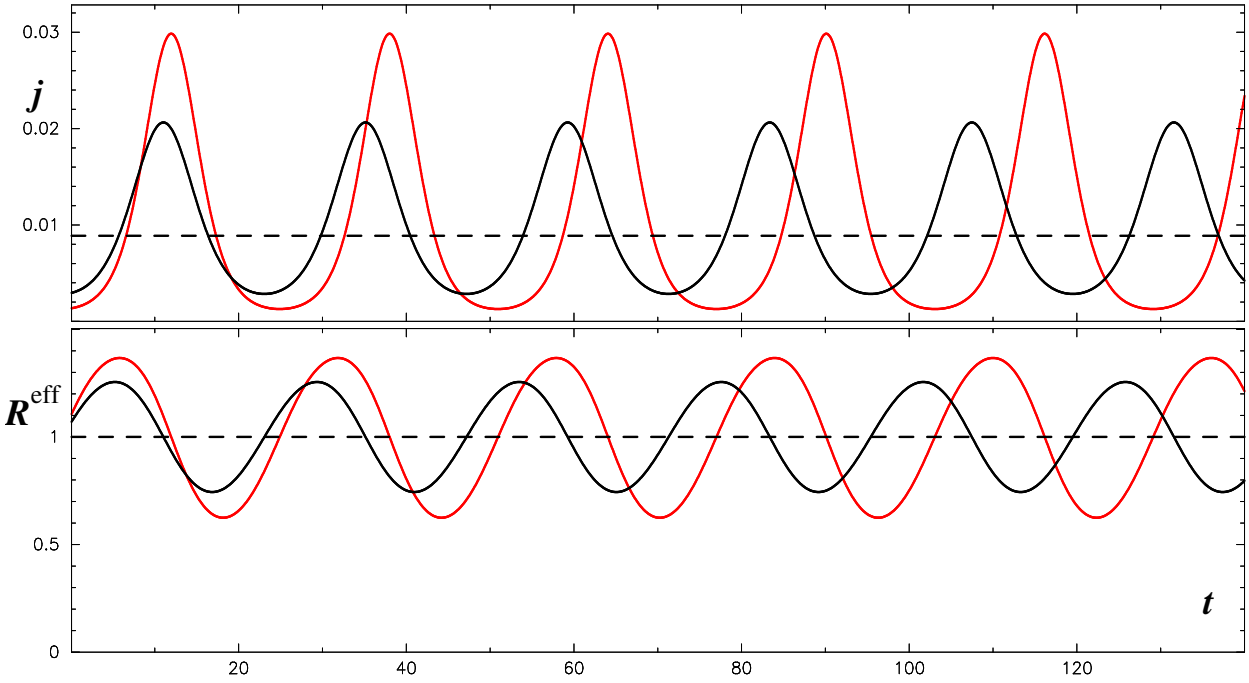


FIG. 4: Same as fig.3 but now for the Erlang distribution with $\xi = 1$, $\eta = 6.5$ (black), and $\eta = 7.0$ (red).

### B. Stochastic model

There exist plenty of possibilities to extend the model considering noisy perturbations coming from the environment. A nearby assumption is that of a fluctuating infection rate which was studied for a SIRS model without memory and therefore without an oscillatory

instability in [7]. To this end we replace $r_0$ in (15) by

$$r_f(t) = r_0\,(1 + \sigma\,\xi(t))$$

where $\xi(t)$ is a Gaussian distributed random variable (white noise) with

$$< \xi(t) >= 0, \qquad < \xi(t)\xi(t') >= \delta(t - t')$$

and $\sigma$ denotes the noise intensity. Thus, the stochastic model reads now

$$ds = \left[-\frac{r_0\,j\,s}{f(j_d)} + \mu\,(1 - j - s)\right]\,dt - \frac{\sigma\,r_0\,j\,s}{f(j_d)}\,dW \tag{24a}$$

$$dj = \left[\frac{r_0\,j\,s}{f(j_d)} - j\right]\,dt + \frac{\sigma\,r_0\,j\,s}{f(j_d)}\,dW\ . \tag{24b}$$

where $dW$ is the one-dimensional Wiener process [8] with

$$dW = \xi(t)\,dt\ .$$

A numerical realization of (24) applying a stochastic Euler forward method (Euler-Maruyama scheme) [12] with time step $\delta t$ reads

$$s_{k+1} = s_k + \left[-\frac{r_0\,j_k\,s_k}{f(j_{dk})} + \mu\,(1 - j_k - s_k)\right]\,\delta t - \frac{\sigma\,r_0\,j_k\,s_k}{f(j_{dk})}\,z_k\sqrt{\delta t} \tag{25a}$$

$$j_{k+1} = j_k + \left[\frac{r_0\,j_k\,s_k}{f(j_{dk})} - j_k\right]\,\delta t + \frac{\sigma\,r_0\,j_k\,s_k}{f(j_{dk})}\,z_k\sqrt{\delta t}\ . \tag{25b}$$

where $j_k = j(k\delta t),\ j_{dk} = j_d(k\delta t),\ s_k = s(k\delta t)$ and $z_k$ is a Gaussian or Bernoulli distributed uncorrelated random variable with mean zero and variance one,

$$< z_k >= 0, \qquad < z_k z_\ell >= \delta_{k\ell} \tag{26}$$

and $\delta_{k\ell}$ denotes the Kronecker symbol. For $\delta t \to 0$, the scheme (25) converges to the Itô stochastic ODE system (24).

### *1. δ-kernel*

We repeat the simulations of sect.IV A, first with the $\delta$-kernel, including now fluctuations. System (25) is integrated numerically. For accuracy reasons we treated the deterministic part again by a 4th order Runge-Kutta scheme with $\delta t = 10^{-3}$. The random variable $z_k$ is

computed by an equally distributed series $z_k = \pm 1$ with probability 1/2, fulfilling (26). The result for $\sigma = 0.075$ is shown in fig.5. A main influence of the noise terms can be seen on the amplitudes of the oscillations. Contrary to the series of fig.3 there is now no distinct difference between the amplitudes of $\tau_0 = 5.2$ and $\tau_0 = 6.2$. The main frequency decreases with increasing delay time for both cases.

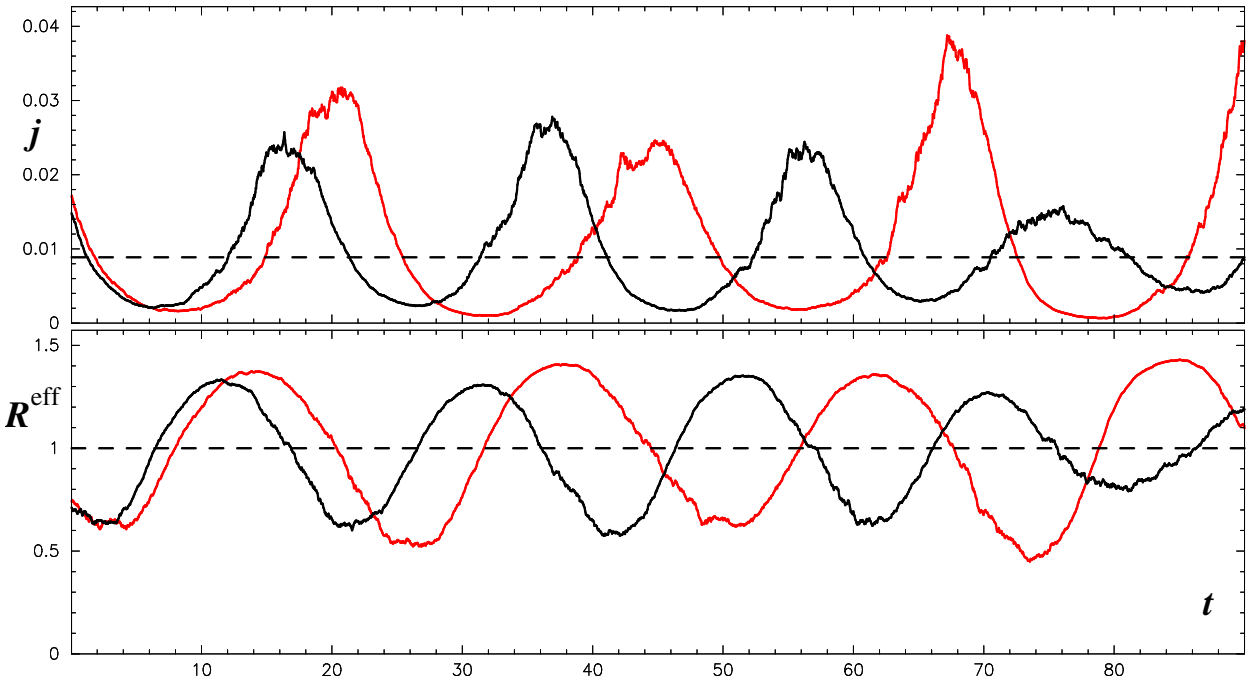


FIG. 5: Infection number and $R^{\text{eff}}$ for the stochastic $\delta$-kernel model with $\sigma = 0.075$, other parameters as in fig.3.

*2. Erlang-kernel*

The same simulations for the Erlang kernel show a significant difference in the behavior of the effective reproduction number, fig.6. Due to the integration over a continuous kernel, $R^{\text{eff}}$ is a smooth function of $t$ and the fluctuations are only pronounced in $j(t)$. For both kernels, the oscillations become much more irregular and the frequencies are distributed over an area with width $\sim \sigma$.

In fig.7 we show the Fourier transform

$$A(\omega_k) = \sum_n^N R^{\text{eff}}(n\delta t) \exp\left(\frac{2\pi i n k}{t_1 - t_0}\right), \qquad \omega_k = 2\pi k/(t_1 - t_0)$$

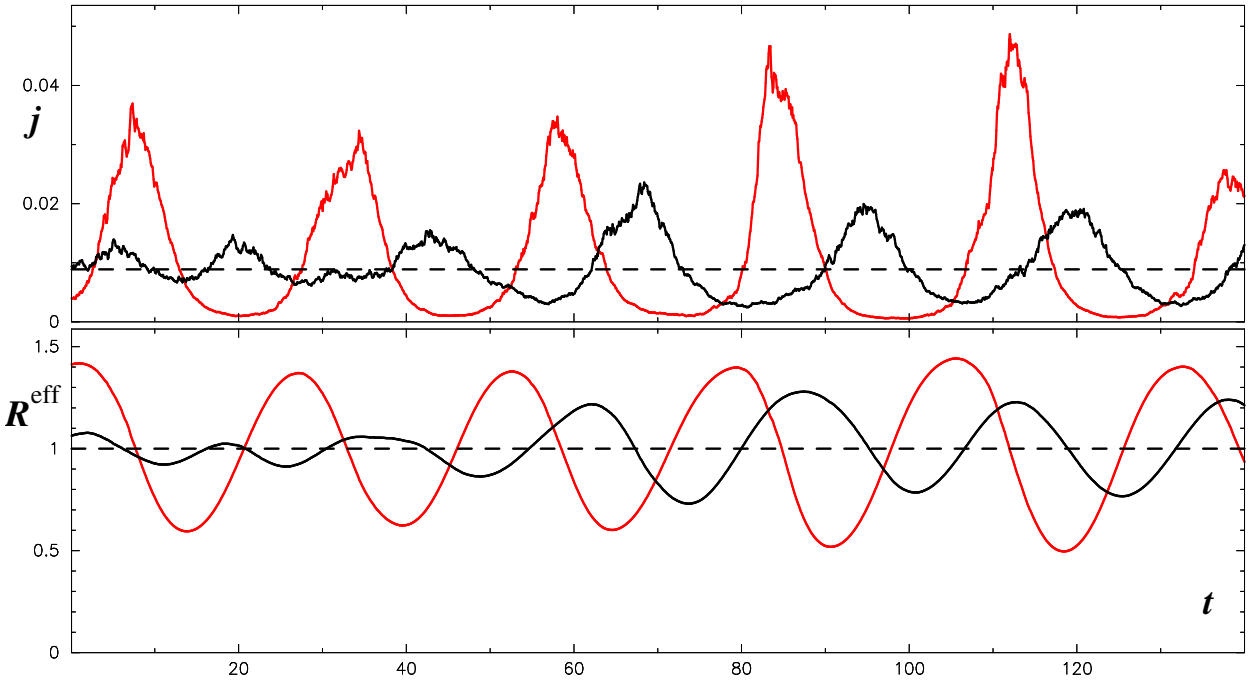


FIG. 6: Infection number and $R^{\text{eff}}$ for the stochastic Erlang kernel model with $\sigma = 0.1$, other parameters as in fig.4.

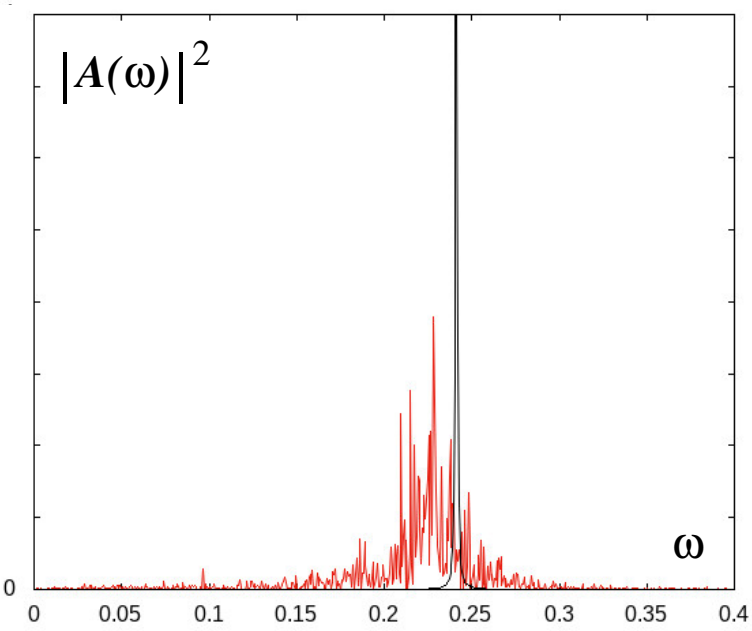


FIG. 7: Fourier transform $|A(\omega)|^2$ (arbitrary units) of a long time series $R^{\text{eff}}(t)$ for $200 < t < 10000$ for the Erlang kernel with $\eta = 7$ and $r_0 = 1.6,\ \alpha = 50,\ \mu = 0.1$. Black: $\sigma = 0$, red: $\sigma = 0.25$.

of a rather long time series up to $t_1 - t_0 = 10000$, corresponding to about 400 oscillations.

The function $R^{\text{eff}}$ is sampled with $N = 2^{16} = 65536$ points with about 160 points per period.

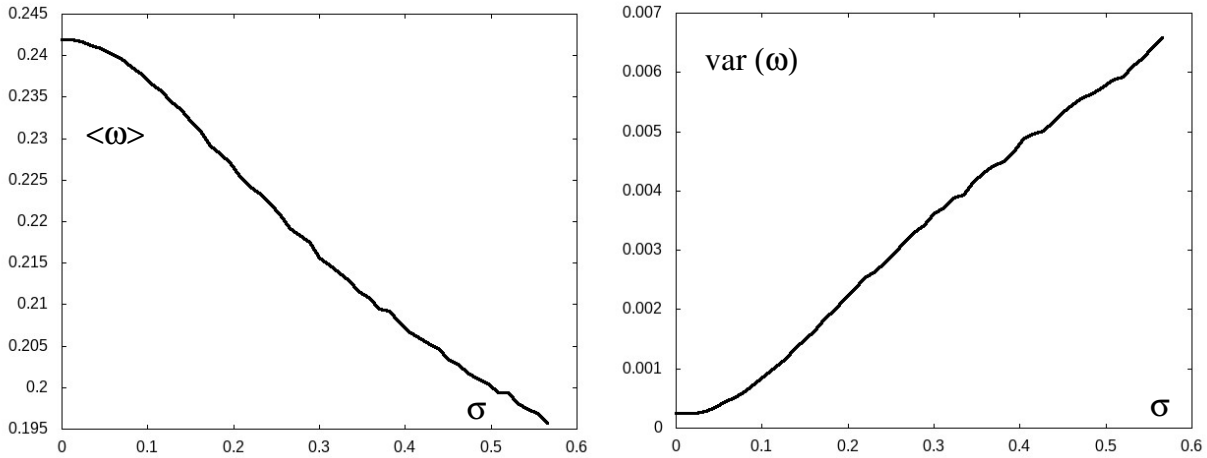


FIG. 8: Mean value (left) and variance of $\omega$ as function of $\sigma$ for the parameters of fig.7. The data is an average over 30 runs with the same parameters but different noise realizations.

Fig.8 shows the mean frequency

$$< \omega >= \frac{1}{N} \sum_k \omega_k \, |A(\omega_k)|^2$$

and the variance

$$\text{var}(\omega) =< \omega^2 > - < \omega >^2$$

over the fluctuation strength $\sigma$. It is clear that for rather large fluctuations the oscillations become very irregular but the main frequency clearly persists, fig.9. We observe that the mean frequency decreases slightly with increasing $\sigma$.

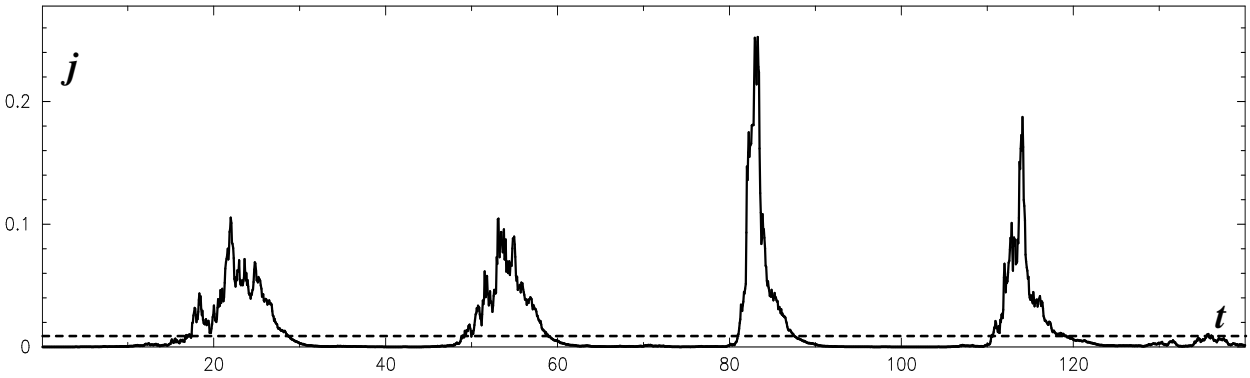


FIG. 9: Infection number for the stochastic Erlang kernel ($\eta = 7$) with large fluctuations $\sigma = 0.6$.

*3. Outbreaks*

For large $\sigma$ the infection dynamics shows long phases where the infection number remains very small, interrupted by sharp periodic bursts, fig.9. The amplitudes of these outbreaks are larger up to a factor 10 than those for the deterministic model (fig.4) and may differ strongly from each other. In this context it is interesting to note that for large $\sigma$, the minimal values for $j(t)$ become very small. For the series with $\sigma = 0.6$ we have $\min(j) \approx 10^{-6}$, for $\sigma = 1$ we find $\min(j) \approx 10^{-9}$. But if the population $N$ is finite, the minimal number of infected individuals according to (4) is $I_m = N \min(j)$. If we take $N \approx 10^8$, corresponding to the population of a rather large country, for $j < 10^{-8}$ there would be no infected individual anymore and the disease would have become extincted. Thus, large fluctuations could lead to extinction even if the basic reproduction number stays larger than one, a result already shown by Cai et al. [2015]. For our model we estimate the critical sigma for extinction with

$$\sigma_c = \frac{\sqrt{2(r_0 - 1)}}{r_0} \ .$$

Not very realistic if for instance compared with data from the recent COVID waves are the rather equal times between the outbreaks. Here it could be possible to include fluctuations also in the immunity loss rate or in the delay times of the feedback control. External effects like seasonal variations could be included as well, a program that we want to study in forthcoming work.

## V. CONCLUSIONS

In this paper we studied the influence of delayed feedback control on the dynamics of a standard SIRS model. Delay terms normally generate oscillatory (Hopf) instabilities of otherwise stable fixed points if the delay time exceeds a certain critical value. Finite time delays, or, for the continuous case, memory effects come into play quite naturally by the rather long time scales of macroscopic effects like a finite time of immunity, the time necessary for the emergence of certain virus mutants, or the time needed to establish mitigation measures. From this list it is clear that there exist many possibilities to extend the model including one or even more memory terms with different kernels. For an upcoming project it could be of interest to study the interplay of two or more different delay terms on an

otherwise low-dimensional deterministic dynamics and see if quasi-periodic or even chaotic solutions may occur. It is known for long that rather simple delay-differential equations like the Mackey-Glass equation [15] or the sinusoidal nonlinearity [26] show chaotic solutions if the time delay becomes large enough.

Further interesting generalizations could be opened by considering fat-tailed memory kernels with power-law decays and with diverging means (very long delay times). Accounting for such kernels leads naturally to time-fractional generalizations of SIR or SIRS models. In particular the combination of random walk models and memory effects induced by renewal processes such as the fractional Poisson process and its generalizations [9, 17, 18, 22] (and many others, see references therein) may be of interest as well.

On the other hand, additional degrees of freedom may be encountered by including environmental noise leading to fluctuating parameters of the SIR or SIRS models. Then, simulations in the frame of stochastic nonlinear differential equations with multiplicative noise come into the focus of attention. The present paper tries to study the combined influence of retarded feedback control and fluctuations due to a coupling to the environment onto the same parameter, namely the infection rate. We found that noise my lead to large fluctuations of amplitude and frequency of the otherwise very regular oscillations provided by the time delayed feedback control alone. In this context, the discussion of a corresponding Fokker-Planck equation of (24) could be of interest. Such an equation was derived for (24) in [7], but for the case without delay terms. Here we would need the extension of the Fokker-Planck theory to delay terms, a task that we shall leave for future work.

Our model can be extended in different directions. A finite duration of being immune can as well be included and modeled by a memory term with another given PDF as done in our recent paper [6]. Spatial effects can be taken into account by including diffusion terms in the infection rate equation or considering the dynamics on small-world networks. Finally, space and time varying infection rates could be introduced to model seasonal variations and density distributions of the population.

---

[1] Anderson, R. M. & May, 1992, R. M., [1992] *Infectious Diseases in Humans*, (Oxford University Press, Oxford).

[2] Basnarkov, L., Tomovski, I., Sandev, T., & Kocarev, L. [2021] "Non-Markovian SIR epidemic spreading model", *arXiv:2107.07427*.

[3] Bestehorn, M., Grigorieva, E. V., & Kaschenko, S. A. [2004] "Spatio-temporal structures in a model with delay and diffusion", *Phys. Rev.***E 70**, 026202.

[4] Bestehorn, M. [2018] *Computational Physics*, (De Gruyter Berlin/Boston).

[5] Bestehorn, M., Riascos, A. P., Michelitsch, T. M., & Collet, B. A. [2021] "A Markovian random walk model of epidemic spreading", *Continuum Mech. Thermodyn.* **33**, 1207.

[6] Bestehorn, M., Michelitsch, T. M., Collet, B. A., Riascos, A. P., & Nowakowski, A. F. [2022] "Simple model of epidemic dynamics with memory effects", *Phys. Rev.* **E 105**,024205.

[7] Cai, Y., Kang, Y., Banerjee, M., & Wanga, W. [2015] "A stochastic SIRS epidemic model with infectious force under intervention strategies", *J. Differential Equations***295**, 7463.

[8] Gardiner, C. [2009] *Stochastic Methods: A Handbook for the Natural and Social Sciences*, (Springer, 4th ed.).

[9] Granger, T., Michelitsch, T. M., Bestehorn, M., Riascos, A. P., & Collet, B. A. [2026] "Four compartment epidemic model with retarded transition rates", *Preprint: arXiv:2210.09912*, submitted.

[10] Hutchinson, G. E. "Circular causal systems in ecology", *N.Y. Acd. Sci.***50**, 221.

[11] W.O. Kermack, W. O. & McKendrick, A. G., [1927] "A contribution to the mathematical theory of epidemics", *Proc. Roy. Soc.* **A 115**, pp. 700–721.

[12] Kloeden, P. E. & Platen, E. [1992] *Numerical Solution of Stochastic Differential Equations*, (Springer Berlin).

[13] Liu, W., Levin, A.,& Iwasa, Y. [1986]"Influence of nonlinear incidence rate upon the behavior of SIRS epidemiological models", *J. Math Biol.***23**, 187.

[14] Lotka, A. J. [1998] *Analytical Theory of Biological Populations*, (Plenum Press New York)

[15] Mackey, D. & Glass, L. [1977] "Oscillations and chaos in physiological control systems", *Science***197**, 28.

[16] Martcheva, M., [2015] *An Introduction to Mathematical Epidemiology*, (Springer).

[17] Metzler, R. & Klafter, J. [2000] "The Random Walk's Guide to Anomalous Diffusion : A Fractional Dynamics Approach", *Phys. Rep.***339**, 1-77.

[18] Michelitsch, T.M., Polito, F., & Riascos, A. P. [2021] "On discrete time Prabhakar-generalized fractional Poisson processes and related stochastic dynamics, *Physica***A 565**, 125541.

[19] Pastor-Satorras, R. & Vespignani, A. [2001] "Epidemic dynamics and endemic states in complex networks", *Phys. Rev.* **E 63**, 066117.

[20] Riascos, A. P. & Mateos, J. L. [2021] "Random walks on weighted networks: a survey of local and non-local dynamics", *J. Complex Networks* **9**, cnab032.

[21] Rihan, F. A. [2021] *Delay Differential Equations and Applications to Biology*, (Springer Nature Singapure).

[22] Sandev, T., Metzler, R., & Chechkin, A. [2018] "From Continuous Time Random Walks to the Generalized Diffusion Equation", *Fract. Calc. Appl. Anal.***21**, 10-28.

[23] Small, M. & Tse, C. K. [2005] "Small World and Scale Free Model of Transmission of SARS",*Int. J. Bifurcation Chaos***15**, 1745-1755.

[24] Small, M., Tse, C. K., Walker, D. M. [2006] "Super-Spreaders in the Rate of Transmission of the SARS Virus",*Physica D***215**, 146-158.

[25] Soper, H. E. [1929] "The interpretation of periodicity in disease prevalence", *J. R. Stat. Soc.***92**, 34.

[26] Sprott, J. C. [2007] "A simple chaotic delay differential equation", *Phys. Lett.***A 366**, 397.

[27] Tang, Y., Huang, D., Ruan, S., & Zhang, W. [2008] "Coexistence of limit cycles and homoclinic loops in a SIRS model with a nonlinear incidence rate", *SIAM J. Appl. Math.***69**, 621.

[28] Xiao, D. & Ruan, S. [2007] "Global analysis of an epidemic model with nonmonotonic incidence rate", *Math. Biosci.***208**, 419.